Sparse Game Changers Restore Collective Motion in Panicked Human Crowds

Ajinkya Kulkarni,[1] Sumesh P. Thampi,[2,*] and Mahesh V. Panchagnula[1,†]
[1]Department of Applied Mechanics, Indian Institute of Technology Madras, Chennai 600036, India
[2]Department of Chemical Engineering, Indian Institute of Technology Madras, Chennai 600036, India

(Received 1 November 2017; revised manuscript received 4 November 2018; published 30 January 2019)

Using a dynamic variant of the Vicsek model, we show that the emergence of disorder from an orderly moving human crowd is a nonequilibrium first-order phase transition. We also show that this transition can be reversed by modifying the dynamics of a few agents, deemed as game changers. Surprisingly, the optimal placement of these game changers is found to be in regions of maximum local crowd speed. The presence of such game changers is effective owing to the discontinuous nature of the underlying phase transition. Thus our generic approach provides strategies to (i) delay crowd crush and (ii) design safe evacuation procedures, two aspects that are of paramount importance in maintaining safety of mass gatherings of people.

DOI: 10.1103/PhysRevLett.122.048002

The Kumbh Mela in India [1,2] and the Hajj in Arabia [3–5] are the two biggest periodic human gathering events on Earth. Estimates have shown that $\sim 10^6$–10^7 people gather in a confined space during these events. The dynamics of such large crowds and its possible spontaneous transition to a crush have perplexed researchers for over 30 years. Gatherings at a carnival, in a sports stadium, or at a train station are no less susceptible to crowd disasters [6]. Such transitions are a matter of grave concern to both law enforcement and public health. We study these phase transitions from an orderly movement to a disordered state in large confined mobile crowds with the motive of proposing a control strategy to delay the onset of crush, a state characterized by asphyxia inducing high crowd pressures, and more desirably, to reverse the disordered state back to ordered motion.

The social-force-based model introduced by Helbing and Molnár [7] and its variants have been shown to be capable of describing the emergent dynamics in human crowds [8–12]. Most of these previous studies have relied on a combination of theory and agent-based simulations to study escape dynamics and evacuation efficiency of crowds through narrow openings [7]. Such approaches are now being complemented by on site computer vision studies [4,6], cognitive science [13], and data analytics [14,15]. For example, deployment of authority figures in escaping crowds in a metro station [16], placement of obstacles near the escaping door [17,18], and mixing individualistic and herding behavior [8] are being proposed as means to enhance evacuation efficiency. Of course, analysis of these specific situations and mechanisms to avoid crowd disasters [8,9,11,19] have led us to an understanding of the underlying dynamics. However, it is more promising if we can generalize the physics and use this knowledge to devise strategies to control crowd behavior.

Indeed, in this Letter, we show that such a generalized approach towards crowd control is possible. Figure 1 summarizes the main findings of this Letter. We model a human crowd in the framework of active matter [8,20,21]

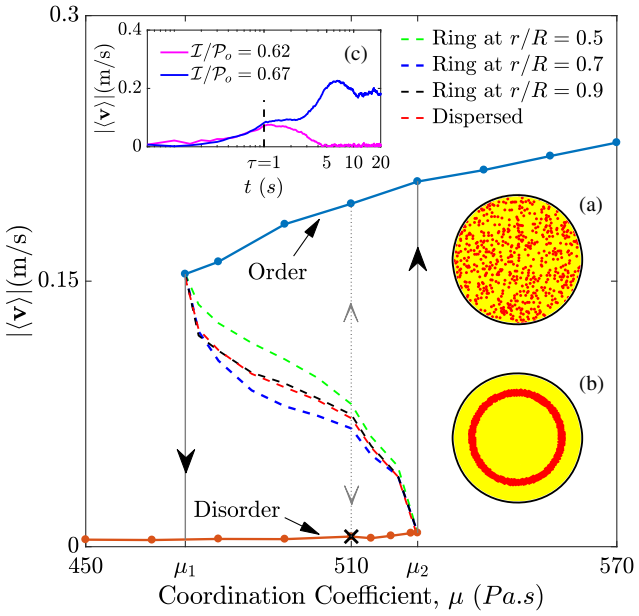

FIG. 1. Bifurcation diagram showing the states of dynamical order and disorder in a human crowd. As the coordination coefficient μ between agents decreases, a uniformly moving crowd with a nonzero average velocity $|\langle \mathbf{v} \rangle|$ loses order, with $|\langle \mathbf{v} \rangle| \approx 0$. Error bars are smaller than symbol height. Insets (a) and (b) show two different choices of location of game changers as red points among other agents marked as yellow. Inset (c) shows a measure of success (finite $|\langle \mathbf{v} \rangle|$ as $t \to \infty$) and failure ($|\langle \mathbf{v} \rangle| \to 0$ as $t \to \infty$) for a given impulse $\mathcal{I}$ compared to the time-averaged momentum in the ordered state $\mathcal{P}_o$ for the value of μ marked with $\times$. The separatrices delineating domains of attraction towards the ordered and disordered states are shown by dashed lines.

and obtain two distinct crowd states, namely, an ordered state of collective motion and a disordered state, which can lead to crush. The ordered state with a nonzero average velocity $|\langle \mathbf{v} \rangle|$ is realized when coordination among the agents is high. Here, $\langle \cdot \rangle$ denotes the average over all agents and over time. A transition to a disordered state where $|\langle \mathbf{v} \rangle| \approx 0$ is observed when agent coordination breaks down. We will show that transition from a collective ordered motion to a state of disorder happens as a nonequilibrium phase transition. More importantly, we find that this transition can be reversed, without requiring a change in the overall level of coordination, by imparting an impulse to a small fraction of agents chosen as "game changers" (GCs). As we will show, GCs work best when they are placed in regions of maximum crowd speed (or lowest local panic). We now describe the model, the implications of these findings for the safety of a human crowd, and the general rationale for optimal game changer placement.

Model description.—We use a dynamical variant of the well-studied agent-based Vicsek model [8,21] to simulate crowd dynamics. This is an off-lattice model, where N agents confined in a circular boundary are modeled as having a mass m, each occupying an area of a soft disk of diameter d. The momentum balance for an ith agent can be written as

$$m\frac{d\mathbf{v}_i}{dt} = \mathbf{F}_i^{pp} + \mathbf{F}_i^{\mathrm{sp}} + \mathbf{F}_i^{D}, \tag{1}$$

where $\mathbf{F}_i^{pp}$, $\mathbf{F}_i^{\mathrm{sp}}$, and $\mathbf{F}_i^{D}$ represent, respectively, the sum of all repulsive forces on the agent due to binary interactions with neighboring agents, a self-propelling force generated by the agent, and an alignment force on the agent due to agent-neighbor interactions. Agent inertia, which is not part of the classical Vicsek model [21] is included in Eq. (1). The repulsive interaction force between the ith agent and a neighboring jth agent occurs due to space exclusion and is modeled as a linear soft spring: $\mathbf{F}_i^{pp} = \sum_j -k_s \mathcal{R}_{ij} \mathcal{H}(|\mathbf{r}_i - \mathbf{r}_j| - d)$. Here, $\mathcal{H}(\cdot)$ is the Heaviside function. If the position vector $\mathbf{r}_i$ points to the center of the ith agent, the extent of compression $\mathcal{R}_{ij}$ is the vectorial distance along the separation vector between two agents i and j. The coefficient k_s determines the strength of the space exclusion force [22,23]. The self-propelling force $\mathbf{F}_i^{\mathrm{sp}}$, produced by an agent has two components: one component aligned with the instantaneous velocity direction $\hat{\mathbf{v}}_i$ of strength β and a second along a predetermined motive direction $\hat{\mathbf{v}}_i^m$ of strength γ. Mathematically, $\mathbf{F}_i^{\mathrm{sp}} = m(\beta\hat{\mathbf{v}}_i + \gamma\hat{\mathbf{v}}_i^m) - \alpha|\mathbf{v}_i|\hat{\mathbf{v}}_i$, where $|\hat{\mathbf{v}}_i| = |\hat{\mathbf{v}}_i^m| = 1$. α is responsible for limiting the agent to a terminal speed [24]. The last force in the list is the collective crowd influence force experienced by each agent and is given by $\mathbf{F}_i^{D} = -\mu d(\mathbf{v}_i - \mathbf{v}_c)$, where μ is a coordination coefficient that controls the coupling strength between the ith agent and its neighborhood crowd, in turn limiting an agent's speed in a dense crowd. We calculate $\mathbf{v}_c$ from a Gaussian weighted average of the velocities of all neighborhood agents in a radius h [22,23], chosen appropriately for dense crowds [5,25]. Notice the absence of extrinsic noise in Eq. (1), unlike previous variants of the Vicsek model [20,21,26].

We consider $N = 6120$ active agents of diameter $d = 0.5$ m confined in a domain of circular shape of radius $R = 22.5$ m and mass $m = 60$ kg, which results in a crowd density $\rho \approx 4$ m^{-2} as observed in typical crowd conditions [27]. We select $k_s = 3 \times 10^6$ N m^{-1} and $\beta = 1$ m/s^2. Typical agent speeds in the simulations match those observed in literature [14,28]. We have set $\alpha = \gamma = 0$ as a model for a dense crowd with low extrinsic motivation [13,14], though $\gamma \neq 0$ will be investigated later to explore the effect of game changers. The conclusions remain robust for $\alpha, \gamma \neq 0$ as well as for polydisperse systems (see [26,29]).

Dynamic states and phase transition.—Two dynamically stable states of the system are obtained from our simulations. They are described by Fig. 2 (see Supplemental Material [26] for videos). At high values of the coordination coefficient μ, active agents organize into an ordered velocity field [see Figs. 2(a) and 2(c)]. This velocity field is azimuthal

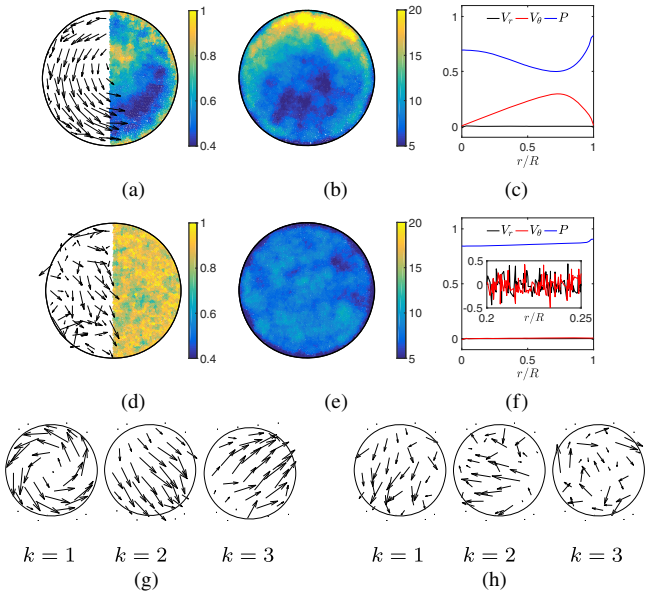

FIG. 2. Instantaneous fields of (a) agent velocity (left half) and panic factor P (right half), (b) crowd pressure (Pa m^{-1}), and (c) a plot of the radial velocity component $V_r = \langle \mathbf{v} \cdot \hat{\mathbf{e}}_r \rangle_{\theta,t}$, the azimuthal velocity component $V_\theta = \langle \mathbf{v} \cdot \hat{\mathbf{e}}_\theta \rangle_{\theta,t}$, and panic factor P versus r/R for a system exhibiting ordered motion at $\mu = 540$ Pa s. Here $\langle \cdot \rangle_{\theta,t}$ is a temporal and azimuthal average. Corresponding plots (d)–(f) for the disordered state at $\mu = 510$ Pa s are shown. The inset of (f) shows the instantaneous velocity profiles. (g),(h) Respectively, the first three dominant modes ($k = 1$–3) of the velocity fields in the ordered and disordered states shown in (a) and (d).

component dominant. The local orientation of this ordered velocity field is determined by the geometry of the confinement similar to other active systems [30–32] as well as in periodic domains [26,33] similar to Refs. [34,35] discussed in [26]. It is not surprising to find giant number fluctuations (GNFs) in an active system [20], but we have an interesting variant—the agent number density exhibits a spatially dependent GNF behavior in the rotary state due to the velocity heterogeneity induced by confinement [26]. From this state, as μ is reduced, collective motion disappears, the order in the velocity field is lost, and we obtain a disordered state [see Figs. 2(d) and 2(f)]. In the disordered state, the thrust force by each agent is balanced by the drag force $m\beta \sim \mu d|\mathbf{v}_i|$, resulting in individual agent speed $|\mathbf{v}_i| \sim (m\beta/\mu d)$ [26].

In order to describe the transition from an individual choice regime to a crowd dominated choice regime, Helbing *et al.* [8] have postulated a "panic factor" P. Casting their equations in our form, we identify the panic factor as

$$P = \frac{m\beta}{m\beta + \mu d|\mathbf{v}_c|}. \tag{2}$$

Thus, panic factor is a ratio of individualistic to the neighboring crowd collective behavior. In a panicked state, agents exhibit individualistic behavior and self-propelling force will exceed the coordination force since $\mathbf{v}_c \approx 0$. Then $m\beta \gg \mu d|\mathbf{v}_c|$ and $P \approx 1$. On the other hand, when the crowd is in an ordered state, the self-propelling force of individual agents would be just sufficient to match the forces exerted by the neighboring crowd: $m\beta \approx \mu d|\mathbf{v}_c|$ and $P \approx \frac{1}{2}$. Since $\mathbf{v}_c$ is a local quantity, Eq. (2) is a generalization of the constant panic factor postulated by Helbing *et al.* [8], thereby allowing the crowd to have spatially varying choices. The panic factors corresponding to the ordered and disordered states are shown in Figs. 2(a) and 2(d), respectively. As expected, $P \approx 1$ in the disordered state as opposed to $P \approx \frac{1}{2}$ in spatial regions of high order. The azimuthally averaged panic factors corresponding to the two states are also shown in Figs. 2(c) and 2(f). Notably, $\frac{1}{2} \leq P \leq 1$ in Fig. 2(c).

In order to quantitatively describe these two states, we define the magnitude of the averaged velocity of the crowd,

$$|\langle \mathbf{v} \rangle| = \sqrt{\left[\frac{1}{T}\int_0^T \frac{1}{N}\sum_i (\mathbf{v}_i \cdot \hat{\mathbf{e}}_r)dt\right]^2 + \left[\frac{1}{T}\int_0^T \frac{1}{N}\sum_i (\mathbf{v}_i \cdot \hat{\mathbf{e}}_\theta)dt\right]^2}$$

as the order parameter. Here, $\hat{\mathbf{e}}_r$ and $\hat{\mathbf{e}}_\theta$ are the unit vectors in the (r, θ) coordinate directions. Another possible choice based on the rotational motion is discussed in the Supplemental Material [26]. Figure 1 shows the variation of $|\langle \mathbf{v} \rangle|$ as a function of μ for a fixed active forcing β and crowd density ρ. At large values of μ, where collective motion dominates, the average velocity $|\langle \mathbf{v} \rangle|$ of the crowd is weakly dependent on μ. The collective motion persists even when μ is lowered but only up to a critical value μ_1. At μ_1 there is a sharp decrease in the order parameter, indicating a phase transition. Collective motion disappears and the agents exhibit diffusive motion. Further reduction in μ maintains $|\langle \mathbf{v} \rangle| \approx 0$. Reversing the experiment by increasing the value of μ gives a different μ_2 for the reverse transition preceded by an active jammed state [26,36,37].

Crowd crush.—Crush is characterized by asphyxia inducing high crowd pressures, which result either from collective motion of agents towards a fixed barrier [38] or due to local velocity disorder [14]. We now examine the threat of crush formation in the two states that we have identified above by (i) studying the eigenmodes of the agents' velocity field [26,38] and (ii) calculating the crowd pressure [13,39]. In the ordered state, the most dominant mode ($k = 1$) in the velocity field is, not surprisingly, ordered rotation [see Fig. 2(g)]. $k = 2, 3$ modes correspond to collective rectilinear movement in orthogonal directions. These two modes, where the agents collectively move towards a boundary, can result in a crush. This threat is also visible by analyzing the crowd pressure in Fig. 2(b), where a region of instantaneous high crowd pressure near the confining wall can be observed. On the other hand, in the disordered state, the two most dominant modes, $k = 1, 2$, [see Fig. 2(h)] correspond to long-range correlated motion against a confining boundary that can lead to crush. Moreover, another mechanism for crowd crush threat is present in the disordered state—large velocity fluctuations that result in local spots of high crowd pressure [14]. While the possibility for crush occurs in both the ordered and disordered states, the disordered state is more alarming considering that evacuation becomes difficult owing to disordered agent motion.

Safety: Recovery from disorder via an induced transition.—So far, we analyzed the order-disorder transition of a crowd using μ as the control parameter. However, as Fig. 1 indicates, the system exhibits hysteresis. An interesting outcome of this observation is that two distinct stable dynamical states exist for $\mu_1 \leq \mu \leq \mu_2$. This presents an opportunity to investigate recovering order from a disordered state.

We start by considering a system exhibiting a state of disorder in the hysteresis region, e.g., the point marked as "×" in Fig. 1. As can be seen, there also exists a state of order at this μ. We now empower GCs in the system and study whether the system can be driven to an ordered state. GCs can be temporary agents either employed at these locations *a priori* or they can be promoted agents. The distribution of GCs can be selected in several ways; we discuss two of them here: GCs uniformly dispersed throughout the domain [Fig. 1(a)] and located in a stripe at various radial locations [Fig. 1(b)].

An impulse $\mathcal{I} = N_g m\gamma\tau$ is imparted to the system in a state of disorder through $N_g (= 10\% N)$ GCs by assigning them a tangential motive force $m\gamma$ for an interval of time τ. For the rest of the crowd, $\gamma = 0$. The response of the system to varying $\mathcal{I}$ corresponding to the point marked × in Fig. 1 is shown as an inset (c) in the same figure. It may be seen

that $|\langle \mathbf{v} \rangle|$ steadily increases for $t > \tau$ when $\mathcal{I}/\mathcal{P}_o \geq 0.67$, indicating spontaneous restoration of order in the system. Here $\mathcal{P}_o = Nm|\langle \mathbf{v} \rangle|_o$ is the total momentum in the ordered state and $|\langle \mathbf{v} \rangle|_o$ is the average velocity in the ordered state. It is interesting to note that GCs do not induce additional crowd pressure during the process of restoring order [26]. On the other hand, when $\mathcal{I}/\mathcal{P}_o < 0.67$, $|\langle \mathbf{v} \rangle|$ reduces towards zero for $t > \tau$. This implies that the system fails to recover from disorder, despite the impulsive forcing.

Successful recovery of the system from a state of disorder depends upon (i) the strength of the impulse ($\mathcal{I}$) provided by GCs and (ii) the location and distribution of GCs (for, e.g., stripe versus dispersed). For $\mu_1 \leq \mu \leq \mu_2$, we have systematically identified the minimum value of $\mathcal{I}$ for which transition to order is achieved, for $(N_g/N) = 0.1$ and any distribution of GCs. Thus, we obtain the separatrices, in Fig. 1 shown as dotted lines, that the GCs have to move the system to, before spontaneous transition to the ordered state sets in. When the system is impulsively forced to an order parameter value above (below) this curve, GCs succeed (fail) in recovering order. As μ increases, $|\langle \mathbf{v} \rangle|$ (and thus the corresponding impulse) required for the system to transit to an ordered state decreases. We also note that the separatrix that lies closest to the disordered state is for the case where the GCs are distributed on a ring located at ≈70% radius of the domain.

In other words, locating GCs at 70% of the domain radius is the optimal way to recover from a disorder in a circular domain without changing the level of coordination between the agents—a result independent of the domain radius R [see Figs. 3(a) and 3(b) as well as [26]]. At approximately $0.7R$, the azimuthal velocity (V_θ) of the agents and therefore $|\mathbf{v}_c|$, are both at their maxima, as seen in Figs. 2(c) and 3(a). Hence the power input to the system ($\mathcal{I}|\mathbf{v}_c|$) through the organized motion of the GCs is maximum. Therefore, the impulse required to transform the system is minimum when they are placed at the locations of maximum crowd speed. Maximum $|\mathbf{v}_c|$ at this location also implies that the panic factor (and thus individualism) is at a minimum.

First-order phase transition and hysteresis.—We now discuss the reasons that lead to the basic premise that the recovery from disorder via GCs is possible and we show that this possibility exists due to the underlying nature of the phase transition. The sharp change in the order parameter in Fig. 3(c) at $\mu = \mu_1, \mu_2$ indicates that the change from an ordered state to a disordered state is a first-order phase transition. We confirm this by calculating the Binder cumulant of the order parameter through the transition while moving to a state of order from a state of disorder. We define the Binder cumulant $G = 1 - [(\langle |\langle \mathbf{v} \rangle_i|^4 \rangle_t)/(3\langle |\langle \mathbf{v} \rangle_i|^2 \rangle_t)]$, following Chaté *et al.* [33] and plot it as a function of the control parameter μ. Here, $\langle \cdot \rangle_i$ denotes average over all agents and $\langle \cdot \rangle_t$ denotes average over time. Figure 3(d) shows this plot for various domain sizes R for a fixed ρ. G varies from 1/3 to 2/3, from a disordered state to an ordered state, as is known for two-dimensional systems. During the transition, the Binder cumulant undergoes a sharp dip at the transition point, proving that crowd disorder is indeed a first-order phase transition from a uniformly moving crowd. Moreover, the size and the sharpness of the dip also increases with an increase in the system size, another feature of a first-order phase transition [33]. Thus, our simulations underscore the discontinuous nature of order-disorder transition seen in Vicsek-like models of active systems [33], additionally under confinement.

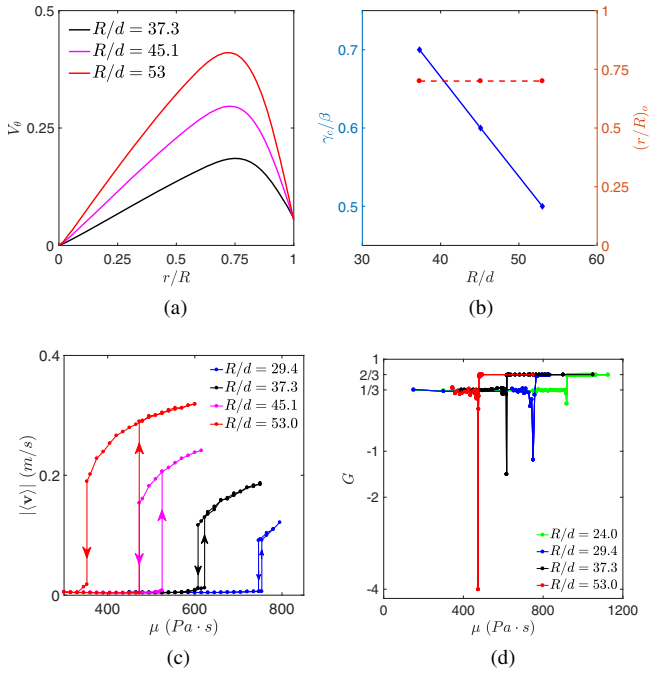

FIG. 3. System size dependence: (a) Profile of V_θ in the ordered phase showing a maximum at $(r/R) \approx 0.7$. (b) The critical impulse γ_c required for transition mediated by GCs and their optimal location. Though the critical impulse required changes with R/d, the optimal location $(r/R)_o$ remains at approximately $0.7R$. (c) During the order-disorder transition (no GCs) in a crowd, the order parameter $|\langle \mathbf{v} \rangle|$ shows a discontinuous change at $\mu = \mu_1, \mu_2$. Different sets correspond to different system sizes. (d) Change in the value of Binder cumulant from 1/3 to 2/3 through a dip at $\mu = \mu_2$ during the transition from disorder to order.

Hysteresis is a hallmark of first-order phase transitions. Therefore, near the transition point, both ordered and disordered states are possible at the same μ. This existence of multiple solutions is the reason for a viable pathway to reverse a disordered state through mobilization of game changers. It appears that the role played by GCs in restoring order is analogous to nucleation in equilibrium phase transitions [40–42]. While nucleation is the route for a first-order phase transition, our analysis also shows that (i) it would not be possible to recover the state through GCs for $\mu < \mu_1$, (ii) there exists an optimal location for the

placement of GCs, and (iii) the width of the hysteresis loop increases with an increase in domain size [see Fig. 3(c)], providing better scope for recovery in case of an accident in larger gatherings.

The authors would like to gratefully acknowledge discussions with Srikanth Vedantam and Silke Henkes.

*sumesh@iitm.ac.in
†mvp@iitm.ac.in

[1] A. Baranwal, A. Anand, R. Singh, M. Deka, A. Paul, S. Borgohain, and N. Roy, PLoS Currents **7** (2015).
[2] I. Barnett, T. Khanna, and J.-P. Onnela, PLoS One **11**, e0156794 (2016).
[3] R. L. Hughes, Annu. Rev. Fluid Mech. **35**, 169 (2003).
[4] S. Kim, S. J. Guy, K. Hillesland, B. Zafar, A. A. -A. Gutub, and D. Manocha, Visual Computer **31**, 541 (2015).
[5] S. Curtis, S. J. Guy, B. Zafar, and D. Manocha, in *Modeling, Simulation and Visual Analysis of Crowds: A Multidisciplinary Perspective*, edited by S. Ali, K. Nishino, D. Manocha, and M. Shah (Springer, New York, 2013), pp. 181–209.
[6] V. J. Kok, M. K. Lim, and C. S. Chan, Neurocomputing; Variable Star Bulletin **177**, 342 (2016).
[7] D. Helbing and P. Molnár, Phys. Rev. E **51**, 4282 (1995).
[8] D. Helbing, I. Farkas, and T. Vicsek, Nature (London) **407**, 487 (2000).
[9] J. Kwak, H.-H. Jo, T. Luttinen, and I. Kosonen, Phys. Rev. E **88**, 062810 (2013).
[10] D. Helbing, A. Johansson, J. Mathiesen, M. H. Jensen, and A. Hansen, Phys. Rev. Lett. **97**, 168001 (2006).
[11] P. Ma and B. Wang, Physica (Amsterdam) **392A**, 215 (2013).
[12] E. N. Cirillo and A. Muntean, Physica (Amsterdam) **392A**, 3578 (2013).
[13] M. Moussaïd, D. Helbing, and G. Theraulaz, Proc. Natl. Acad. Sci. U.S.A. **108**, 6884 (2011).
[14] D. Helbing, A. Johansson, and H. Z. Al-Abideen, Phys. Rev. E **75**, 046109 (2007).
[15] J. L. Silverberg, M. Bierbaum, J. P. Sethna, and I. Cohen, Phys. Rev. Lett. **110**, 228701 (2013).
[16] X. Song, Z. Zhang, G. Peng, and G. Shi, Physica (Amsterdam) **465A**, 599 (2017).
[17] P. Lin, J. Ma, T. Y. Liu, T. Ran, Y. L. Si, F. Y. Wu, and G. Y. Wang, Physica (Amsterdam) **482A**, 228 (2017).
[18] I. Zuriguel, J. Olivares, J. M. Pastor, C. Martín-Gómez, L. M. Ferrer, J. J. Ramos, and A. Garcimartín, Phys. Rev. E **94**, 032302 (2016).
[19] M. Chraibi, A. Seyfried, and A. Schadschneider, Phys. Rev. E **82**, 046111 (2010).
[20] M. C. Marchetti, J. F. Joanny, S. Ramaswamy, T. B. Liverpool, J. Prost, M. Rao, and R. A. Simha, Rev. Mod. Phys. **85**, 1143 (2013).
[21] T. Vicsek, A. Czirók, E. Ben-Jacob, I. Cohen, and O. Shochet, Phys. Rev. Lett. **75**, 1226 (1995).
[22] P. Bonkinpillewar, A. Kulkarni, M. Panchagnula, and S. Vedantam, Granular Matter **17**, 511 (2015).
[23] P. S. Mahapatra, A. Kulkarni, S. Mathew, M. V. Panchagnula, and S. Vedantam, Phys. Rev. E **95**, 062610 (2017).
[24] D. F. Hinz, A. Panchenko, T.-Y. Kim, and E. Fried, Soft Matter **10**, 9082 (2014).
[25] C. Bechinger, R. Di Leonardo, H. Löwen, C. Reichhardt, G. Volpe, and G. Volpe, Rev. Mod. Phys. **88**, 045006 (2016).
[26] See Supplemental Material at http://link.aps.org/supplemental/10.1103/PhysRevLett.122.048002 for additional information pertaining to dominant eigenmodes, inter-particle and swim pressure, the effect of polydispersity as well as Giant Number Fluctuations (GNF). Videos of the simulations are also included.
[27] D. R. Parisi, M. Gilman, and H. Moldovan, Physica (Amsterdam) **388A**, 3600 (2009).
[28] G. Baglietto and D. R. Parisi, Phys. Rev. E **83**, 056117 (2011).
[29] P. Mahapatra, S. Mathew, M. Panchagnula, and S. Vedantam, Granular Matter **18**, 30 (2016).
[30] H. Wioland, F. G. Woodhouse, J. Dunkel, J. O. Kessler, and R. E. Goldstein, Phys. Rev. Lett. **110**, 268102 (2013).
[31] E. Lushi, H. Wioland, and R. E. Goldstein, Proc. Natl. Acad. Sci. U.S.A. **111**, 9733 (2014).
[32] A. Czirók, E. Ben-Jacob, I. Cohen, and T. Vicsek, Phys. Rev. E **54**, 1791 (1996).
[33] H. Chaté, F. Ginelli, G. Grégoire, and F. Raynaud, Phys. Rev. E **77**, 046113 (2008).
[34] P. Romanczuk, I. D. Couzin, and L. Schimansky-Geier, Phys. Rev. Lett. **102**, 010602 (2009).
[35] F. Ginelli and H. Chaté, Phys. Rev. Lett. **105**, 168103 (2010).
[36] S. Banerjee, K. J. C. Utuje, and M. C. Marchetti, Phys. Rev. Lett. **114**, 228101 (2015).
[37] S. Henkes, Y. Fily, and M. C. Marchetti, Phys. Rev. E **84**, 040301 (2011).
[38] A. Bottinelli, D. T. J. Sumpter, and J. L. Silverberg, Phys. Rev. Lett. **117**, 228301 (2016).
[39] S. C. Takatori, W. Yan, and J. F. Brady, Phys. Rev. Lett. **113**, 028103 (2014).
[40] K. Binder, Rep. Prog. Phys. **50**, 783 (1987).
[41] P. C. Hohenberg and J. B. Swift, Phys. Rev. E **52**, 1828 (1995).
[42] L. P. Csernai and J. I. Kapusta, Phys. Rev. D **46**, 1379 (1992).